Synthesis of hydroxycinnamic acid glucuronides and investigation of their affinity for human serum albumin†

Stéphanie Galland, Njara Rakotomanomana, Claire Dufour, Nathalie Mora and Olivier Dangles*

Received 12th June 2008, Accepted 16th September 2008
First published as an Advance Article on the web 8th October 2008
DOI: 10.1039/b809965k

Hydroxycinnamic acids (HCAs) are among the most abundant dietary polyphenols. Recent bioavailability studies have shown that HCAs enter the blood circulation mainly as glucuronides, which are thus most likely to express their potential health effects. In this work, an efficient synthesis of HCA *O*-arylglucuronides is developed. As for many xenobiotics, the resilience of HCA *O*-arylglucuronides in plasma and subsequent delivery to tissues could be governed by their binding to human serum albumin (HSA). Hence, the affinity of HCA *O*-arylglucuronides for HSA and its possible binding site were investigated by fluorescence spectroscopy. HCA *O*-arylglucuronides turn out to be moderate HSA ligands (K in the range $1–4 \times 10^4$ M^{-1}) that bind HSA in sub-domain IIA, competitively or noncompetitively with other sub-domain IIA ligands such as dansylamide and the flavonol quercetin.

Introduction

The mean consumption of polyphenols is of the order of 0.5 g per person per day, with hydroxycinnamic acids (HCAs) making one of the highest contributions.[1,2] Hence, investigating the bioavailability of HCAs is of great importance for a better understanding of the potential health effects of polyphenols. In fact, HCAs are diversely absorbed from the gastro-intestinal tract depending on their structure. For instance, chlorogenic acid (5-caffeoylquinic acid), the most abundant caffeic acid derivative in food, can be directly taken up from the gastric compartment of rats.[3] In rats, *p*-coumaric and ferulic acids, but not gallic acid, have been shown to cross the cells of the small intestine *via* the monocarboxylic acid transporter.[4] As for chlorogenic acid, the absorption mechanism (determined *in vitro* with Caco-2 cells) involves removal of the quinic moiety by a mucosa esterase and subsequent absorption of caffeic acid *via* the monocarboxylic acid transporter.[5] However, most of the absorption of chlorogenic acid must take place in the colon after hydrolysis to caffeic acid by bacterial esterases.

After intestinal absorption, HCAs are extensively metabolized in enterocytes and hepatocytes through sulfation and glucuronidation.[6–10] These conjugates can be returned to the gastro-intestinal tract *via* the bile (and partially re-absorbed) or excreted in urine. Glucuronidation catalyzed by UDP-glucuronosyltransferases is the main conjugation pathway. For instance, 2 hours after ingestion of 700 μmol kg^{-1} of pure caffeic acid by rats, the plasma concentration of caffeic acid glucuronides reaches *ca.* 26 μM, *i.e.* more than 40% of the total circulating caffeic acid concentration, whereas the concentrations of free caffeic and ferulic acids do not exceed 1–2 μM.[7] In humans, 1 hour after ingestion of a cup of coffee (*ca.* 1 mmol of caffeic acid), the caffeic acid concentration reaches a maximal value in the range 0.3–1.0 μM after deconjugation by β-glucuronidases whereas concentrations 4–5 times as low are detected in untreated plasma.[8] After consumption of high-bran cereals rich in ferulic acid, ferulic acid glucuronide was detected in plasma as the main metabolite.[9] After beer consumption, ferulic and caffeic acids mainly circulate as sulfates and glucuronides, whereas much higher levels of free *p*-coumaric acid are detected.[10] After tomato consumption by humans, ferulic acid is excreted as a mixture of the free form and glucuronide, and the total recovery amounts to 11–25% of the ingested dose. At the maximal excretion (approximately 7 h after ingestion), the molar ratio of the glucuronide to that of the free form is 2–3 : 1.[11]

Polyphenol metabolites probably circulate in association with plasma proteins. For instance, flavonol conjugates are bound to human serum albumin (HSA), the most abundant plasma protein.[12] Binding of xenobiotics (*e.g.*, drugs, dietary components, toxins) to serum albumin typically modulates the rate of clearance and delivery to tissues.[13] It can also modulate the antioxidant capacity of polyphenols, in particular their ability to inhibit lipid peroxidation in HSA–polyunsaturated fatty acid complexes and in low-density lipoproteins.[14,15]

In this work, efficient routes for the chemical synthesis of *O*-arylglucuronides of hydroxycinnamic acids are proposed. The conjugates thus prepared are then tested for their affinity for HSA. Improved data treatments are devised for the determination of binding constants, binding sites and possible multiple binding processes.

Results and discussion

Synthesis of hydroxycinnamic acid *O*-arylglucuronides

Access to well-characterized chemically pure polyphenol conjugates is a critical step toward a better understanding of their bioavailability and cell effects. Indeed, the low concentration of circulating polyphenol metabolites requires comparison with authentic standards for conclusive identification, especially when it comes to distinguishing between regioisomers. For instance, glucuronidation of caffeic acid can yield three regioisomers, one

UMR408 Sécurité et Qualité des Produits d'Origine Végétale, INRA, Université d'Avignon, F-84000, Avignon, France. E-mail: Olivier.Dangles@univ-avignon.fr; Fax: +33 490 14 44 41; Tel: +33 490 14 44 46

† Electronic supplementary information (ESI) available: ^{1}H NMR spectra of hydroxycinnamic acid glucuronides. See DOI: 10.1039/b809965k

acylglucuronide[16] and two arylglucuronides. On the other hand, the bulk of cell studies published up to now has dealt with native polyphenols, typically aglycones, whereas conjugated forms, especially glucuronides, are much more likely to be distributed to tissues.

The synthetic route summarized on Scheme 1 is close to that already developed for the synthesis of **5a**.[17] The key step is the glucuronidation of methyl hydroxycinnamates (**1a–c**) by methyl 2,3,4-tri-*O*-acetyl-1-*O*-(trichloroacetimidoyl)-α-D-glucuronate (**2**) activated by the boron trifluoride–diethyl ether complex in anhydrous dichloromethane at room temperature, which afforded the protected glucuronides (**3a–d**) in moderate to good yields. In the case of methyl caffeate, mixtures of 3′-*O*-β-D-glucuronide (**3d**) and 4′-*O*-β-D-glucuronide (**3c**) were obtained. As expected from the orienting effect of the 2-*O*-acetyl group, the glucuronidation was stereoselective and led to the exclusive formation of the β anomers ($J(H_1–H_2) = 6.9$ Hz). As already observed in our previous work with HCA *O*-arylglucosides,[18] the final cleavage of the acetyl and methylester groups could not satisfactorily be carried out in one step in the ferulic and caffeic series. Indeed, **3b** and **3c–d** had to be deprotected in two steps involving sugar deacetylation by mild catalytic methanolysis (compounds **4b–d**) followed by methyl ester saponification using a stoichiometric amount of NaOH (2 equiv.). All glucuronides were characterized by high-resolution MS and NMR analyses. Glucuronidation at position 4′ for **5c** and at position 3′ for **5d** were deduced from analysis of the chemical shifts of the aromatic protons (glucuronidation lowers the electron-donating effect of the OH group, thus producing a deshielding of the aromatic protons *ortho* and *para* to the glucuronyl group) in comparison with the corresponding aglycones and glucosides.[18]

Binding to HSA

As many other xenobiotics, polyphenols could bind to serum albumin in the blood circulation and form complexes that modulate their resilience in plasma and their delivery to tissues.[12] However, most studies reported up to now[19–22] have dealt with native polyphenols, essentially aglycones, although these forms (when detectable) remain very minor in plasma after ingestion of polyphenol-rich foods or supplements. Indeed, dietary polyphenols typically travel in plasma as glucuronides and sulfates of aglycones as a result of extensive conjugation in the intestinal and liver cells.[1,2] Interestingly, these conjugates themselves could bind to HSA, as already suggested for flavonol conjugates.[12,23] In this work, the preparation of pure hydroxycinnamic acid glucuronides offers a good opportunity to investigate their affinity toward HSA in comparison with the parent aglycones.

Polyphenol–HSA binding can be investigated by a combination of fluorescence techniques.[12,21,24] One method consists of monitoring the fluorescence of the polyphenolic ligand in the presence and absence of HSA. This approach turned out to be disappointing with HCAs for several reasons. First, HCAs in their free or HSA-bound form are poorly fluorescent, so that the relatively large ligand concentrations required make the data treatment more complicated because of lack of linearity in the fluorescence intensity *vs.* concentration plots and possible multiple bindings. Second, in the ferulic and caffeic series, substantial photo-induced *Z–E* isomerization of the carbon–carbon double bond takes place that makes the fluorescence intensity unstable. In fact, only 4-*O*-β-D-glucuronyl-*p*-coumaric acid (**5a**) could be investigated by this method. Indeed, this ligand is much less prone to isomerization,

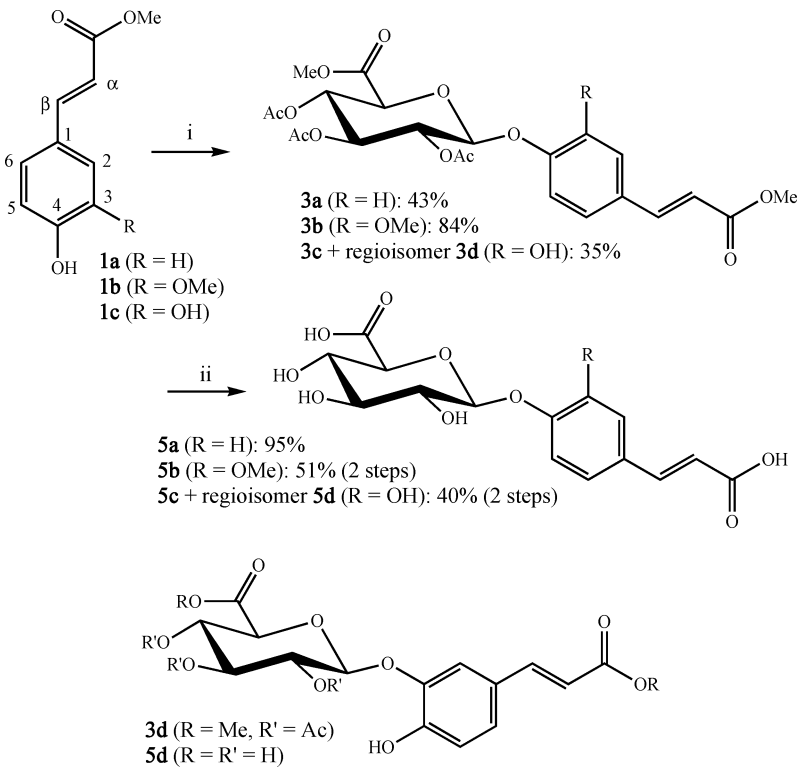

Scheme 1 Organic synthesis of HCA arylglucuronides. *Reagents and conditions*: i) Methyl 2,3,4-tri-*O*-acetyl-1-*O*-(trichloroacetimidoyl)-α-D-glucuronate (**2**, 1–2 equiv.) $BF_3{\cdot}Et_2O$ (1–2 equiv.), CH_2Cl_2; ii) NaOH (8 equiv.) in H_2O–MeOH (1 : 1) (R = H) or MeONa (0.1 equiv.) in MeOH, then NaOH (2 equiv.) in H_2O–MeOH (1 : 1) (R = OH, OMe), followed by final acidification by a proton-exchange resin.

Table 1 Binding of selected ligands to human serum albumin in a pH 7.4 phosphate buffer at 25 °C. Fluorescence monitoring following excitation of the ligand or probe

	$10^{-3}K/M^{-1}$	$10^{-3}f_P/M^{-1}$	$10^{-3}f_{PL}/M^{-1}$	r^2, number of points	λ_{ex}, λ_{em}/nm (ε_L at $\lambda_{ex}/M^{-1}cm^{-1}$)
5[a]	21.9 (± 1.4)	177 (± 1)	348 (± 2)[a]	0.997, 100	335, 430
DNSA	107 (± 2)	27.5 (± 3.2)	851 (± 3)[b]	0.9993, 98	360, 490
DNSS	156 (± 4)	27.7 (± 4.5)	1010 (± 4)[c]	0.9994, 58	360, 490
5a (DNSA)	22.2 (± 0.4)	535 (± 2)[d]	—	0.999, 42	360, 490 (170)
5a (DNSS)	16.2 (± 0.6)	675 (± 4)[d]	—	0.996, 44	360, 490 (170)
5b (DNSA)	4.0 (± 0.1)	620 (± 2)[d]	—	0.997, 56	360, 490 (20)
5b (DNSS)	3.4 (± 0.1)	705 (± 2)[d]	—	0.996, 44	360, 490 (20)
1a (DNSA)	6.2 (± 0.2)	477 (± 2)[d]	—	0.996, 46	360, 490 (290)
1a (DNSS)	8.2 (± 0.2)	661 (± 3)[d]	—	0.997, 58	360, 490 (290)

[a] $f_L = 12.4 \times 10^3$ M^{-1}. [b] $f_L = 4625$ M^{-1}. [c] $f_L = 2420$ M^{-1}. [d] Molar fluorescence of the probe–HSA complex.

and its excitation spectrum (Fig. 1) makes it possible to set the irradiation at a wavelength (335 nm) where absorption is weak (a condition for proportionality between fluorescence intensity and concentration[25]). Consequently, a saturatable binding isotherm could be constructed from which the binding constant (pure 1 : 1 binding assumed) was extracted (Fig. 2, Table 1): $K_1 \approx 22 \times 10^3$ M^{-1}.

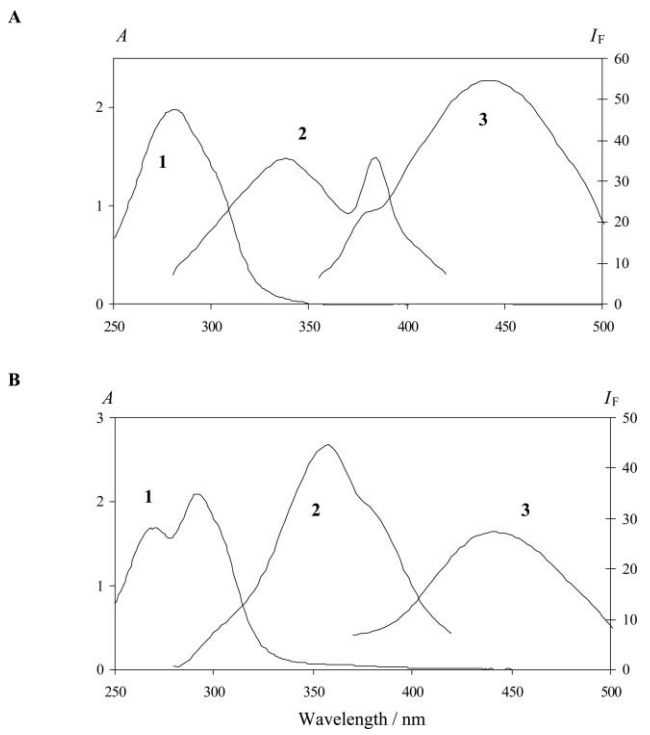

Fig. 1 Absorption (**1**), excitation (**2**) and emission (**3**) spectra of 4-*O*-β-D-glucuronyl-*p*-coumaric acid (**5a**) in the absence (**A**) or presence (**B**) of HSA (pH 7.4 phosphate buffer, 25 °C). Excitation and emission wavelengths are set at 335 and 430 nm, respectively.

For the other ligands, we had to consider the HSA intrinsic fluorescence due to its single Trp residue (Trp-214), which is located in sub-domain IIA where small negatively charged aromatic ligands are most likely to bind.[26] The signal intensity and its sensitivity to quenching by sub-domain IIA binders make it possible to use small protein and ligand concentrations. However, all the selected ligands absorb at the excitation wavelength (295 nm) so that a correction of the fluorescence intensity at 340 nm for this inner filter effect has to be applied in the data treatment (see experimental part and ref. 24). Although acceptable curve-fittings were achieved within the hypothesis of pure 1 : 1 binding, significant improvements were noted in the fitting of the final part of the curves (high ligand concentration) by assuming additional 1 : 2 protein–ligand binding (Fig. 3, Table 2). In the initial calculations, both the 1 : 1 and 1 : 2 complexes are assumed to be nonfluorescent. With **5a**, the K_1 values thus obtained can be compared with the one deduced from the previous method (enhancement of ligand fluorescence: $K_1 \approx 22 \times 10^3$ M^{-1}): $K_1 \approx 14 \times 10^3$ M^{-1} (quenching of Trp fluorescence by pure 1 : 1 binding), $K_1 \approx 10 \times 10^3$ M^{-1} (quenching of Trp fluorescence by 1 : 1 and 1 : 2 bindings). Finally, if we consider that the K_1 value deduced from the enhancement of ligand fluorescence is most reliable because no inner filter correction is required, the best compromise seems to refine the fluorescence quenching data with a K_1 value set constant at 22×10^3 M^{-1} and to assume both 1 : 1 and 1 : 2 bindings and an intermediate fluorescent 1 : 1 complex (molar fluorescence intensity $f_{PL} \neq 0$). A more reliable value for the stepwise 1 : 2 binding constant is thus obtained: $K_2 \approx 13 \times 10^3$ M^{-1}. Hence, HSA seems to display two sites of close affinity for accommodating **5a**. For the other HCAs, such cross-control cannot be carried out since K_1 cannot be independently determined from the ligand fluorescence method. However, for the other glucuronides, a reasonable strategy could be to use the f_{PL} value deduced from L = 4-*O*-β-D-glucuronyl-*p*-coumaric acid and fit the curves with f_P (molar fluorescence intensity of free HSA), K_1 and K_2 as the optimizable parameters (Table 2). As an example, with 4-*O*-β-D-glucuronylferulic acid (**5b**), we obtain: $K_1 \approx 21 \times 10^3$ (1 : 1 binding), 16×10^3 (1 : 1 + 1 : 2 bindings, $f_{PL} = 0$) and 36×10^3 (1 : 1 + 1 : 2 bindings, $f_{PL} \neq 0$) M^{-1}. These small discrepancies reflect the difficulties inherent to quantitatively investigating the binding to serum albumin of relatively small and moderate ligands that can possibly partition over several binding sites, even within the same sub-domain. Anyway, it is comforting to note that the quercetin–HSA binding constant is consistent with previous estimations using a variety of techniques.[19–21] The order of magnitude of the K_1 values for the HCAs (aglycones) is also in general agreement with previous reports.[27,28] Taking the K_1 values deduced from simple 1 : 1 binding as an acceptable scale of relative affinity for HSA, it can be noted that the bulky glucuronyl moiety only moderately lowers the affinity of HCAs for HSA (at most, by a factor of 2).

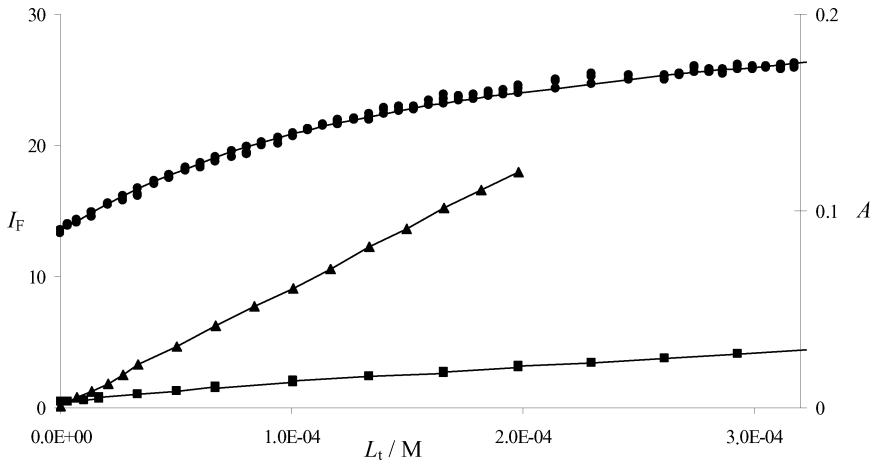

Fig. 2 Changes in the fluorescence intensity of 4-*O*-β-D-glucuronyl-*p*-coumaric acid (**5a**) at 430 nm (λ_{ex} = 335 nm) as a function of its concentration. Initial HSA concentration = 75 μM (pH 7.4 phosphate buffer, 25 °C). Fluorescence of HSA-bound ligand (●) and free ligand (■), absorbance of free ligand at 335 nm (▲).

Table 2 Binding of selected ligands to human serum albumin (3.75 μM) in a pH 7.4 phosphate buffer at 25 °C. Fluorescence monitoring at 340 nm following excitation of HSA (single Trp residue) at 295 nm

Ligand	$10^{-3}K$/M^{-1}	$10^{-5}f_P$/M^{-1}	$10^{-5}f_{PL}$/M^{-1}	r^2, number of points	ε_L(295 nm)/M^{-1} cm^{-1} [a]
1a	39.5 (± 1.3)	95.1 (± 0.7)	—	0.997, 51	14420
1a[b]	28.7 (± 1.7), 14.6 (± 3.0)	93.1 (± 0.5)	—	0.998, 51	
1b	33.6 (± 1.1)	95.9 (± 0.6)	—	0.997, 50	14100
1b[b]	23.4 (± 1.3), 15.6 (± 2.7)	93.6 (± 0.5)	—	0.999, 50	
1c	41.8 (± 0.9)	106.3 (± 0.5)	—	0.998, 54	13110
1c[b]	32.1 (± 0.8), 11.9 (± 1.1)	104.1 (± 0.3)	—	0.9997, 54	
5a	14.1 (± 0.3)	116.8 (± 0.4)	—	0.998, 63	10840
5a[b]	10.1 (± 0.4), 8.3 (± 1.0)	114.9 (± 0.3)	—	0.9995, 63	
5a[c]	21.9[d], 13.2 (± 0.9)	114.6 (± 0.3)	65.9 (± 2.7)	0.9995, 63	
5b	41.8 (± 0.9)	106.3 (± 0.5)	—	0.998, 54	13110
5b[b]	32.1 (± 0.8), 11.9 (± 1.1)	104.1 (± 0.3)	—	0.9997, 54	
5b[c]	35.6 (± 1.2), 17.5 (± 0.6)	114.9 (± 0.2)	66[d]	0.9997, 58	
5c	19.8 (± 0.7)	111.4 (± 0.7)	—	0.997, 59	12850
5c[b]	12.4 (± 0.8), 15.9 (± 2.5)	108.6 (± 0.5)	—	0.999, 59	
5c[c]	26.2 (± 2.5), 22.3 (± 1.9)	108.0 (± 0.5)	66[d]	0.999, 59	
5d	28.7 (± 1.1)	118.5 (± 0.9)	—	0.997, 59	14310
5d[b]	16.3 (± 0.8), 23.3 (± 2.6)	114.7 (± 0.4)	—	0.9994, 59	
5d[c]	30.2 (± 2.2), 34.8 (± 2.2)	113.9 (± 0.4)	66[d]	0.9993, 59	
Quercetin	222.0 (± 4.7)	114.2 (± 0.7)	—	0.999, 45	9410
DNSA	107[d], 12.9 (± 0.6)	112.4 (± 0.5)	52.9 (± 1.1)	0.9993, 63	
DNSS	156[d], 10.1 (± 0.7)	125.8 (± 0.6)	55.7 (± 1.3)	0.999, 56	

[a] Fluorescence intensity corrected by a factor $\exp(-\varepsilon_L l L_t)$ with l = 0.65 cm (L_t: total ligand concentration). [b] 1 : 1 and 1 : 2 bindings (nonfluorescent 1 : 1 and 1 : 2 complexes). [c] 1 : 1 and 1 : 2 bindings (fluorescent 1 : 1 complex, nonfluorescent 1 : 2 complex). [d] Set constant.

The highly sensitive fluorescent probes dansylamide (DNSA) and dansylsarcosine (DNSS) were used for competitive experiments with the HCAs to gain information about substantial differences in binding locations. DNSA is a sub-domain IIA binder whereas DNSS could also partition in sub-domain IIIA.[29] The strategy developed above for 4-*O*-β-D-glucuronyl-*p*-coumaric acid (**5a**) was also applied to the dansyl probes to estimate the values of their 1 : 1 and 1 : 2 binding constants to HSA. Thus, K_1 was accurately determined from the ligand fluorescence method (excitation at 360 nm, emission at 490 nm) and this value was used in the quenching of the Trp fluorescence to estimate K_2 (Tables 1 and 2). Then, the fluorescence of the dansyl probe–HSA complex was gradually quenched by increasing concentrations of **5a**. The quenching curves were analyzed within the hypothesis of pure competitive 1 : 1 binding for both the probe and ligand and by taking into account a very weak inner filter effect due to absorption of the ligand at the excitation wavelength (Fig. 4). These assumptions were nicely validated by the K_1 values thus extracted ($K_1 \approx 22 \times 10^3$ M^{-1} with DNSA, 16×10^3 M^{-1} with DNSS) which are in agreement with our previous estimate ($K_1 \approx 22 \times 10^3$ M^{-1}) (Table 1). Although the K_1 values of the other HCAs are less accurately determined, it can be safely stated that this competitive binding is not a general rule. For instance, the quenching of both DNSS–HSA and DNSA–HSA fluorescence

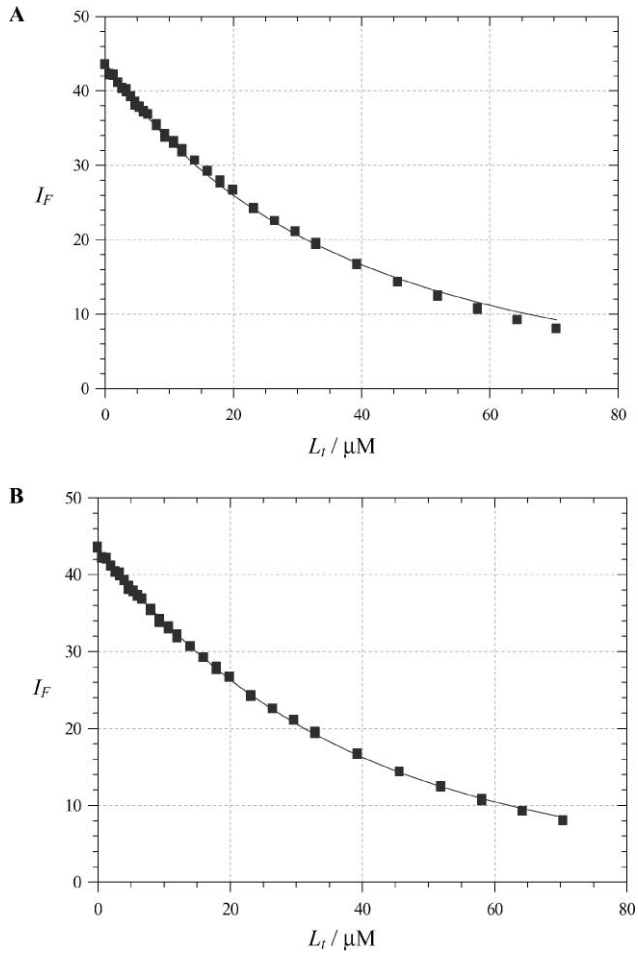

Fig. 3 Changes in the fluorescence intensity of HSA at 340 nm (λ_{ex} = 295 nm) as a function of the 4-*O*-β-D-glucuronylferulic acid (**5b**) concentration (pH 7.4 phosphate buffer, 25 °C). Initial HSA concentration = 3.75 μM. **A**: curve-fitting assuming pure 1 : 1 binding, **B**: curve-fitting 1 : 1 and 1 : 2 bindings.

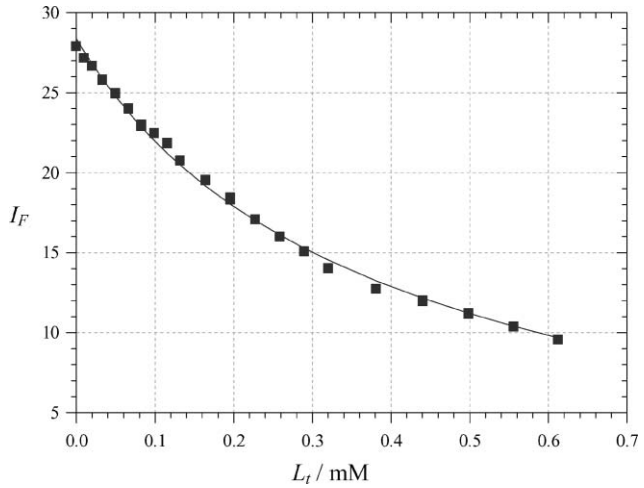

Fig. 4 Changes in the fluorescence intensity of dansylamide at 490 nm (λ_{ex} = 360 nm) as a function of the concentration of 4-*O*-β-D-glucuronyl-*p*-coumaric acid (**5a**). Initial HSA and DNSA concentrations = 75 μM (pH 7.4 phosphate buffer, 25 °C). The solid line is the result of the curve-fitting.

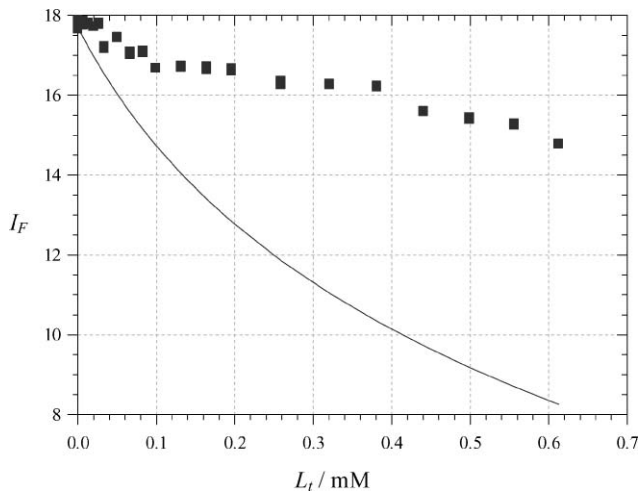

Fig. 5 Changes in the fluorescence intensity of quercetin at 530 nm (λ_{ex} = 450 nm) as a function of the concentration of 4-*O*-β-D-glucuronyl-*p*-coumaric acid (**5a**). Initial HSA and quercetin concentrations = 75 μM (pH 7.4 phosphate buffer, 25 °C). The solid line is the result of a simulation assuming competitive binding.

by *p*-coumaric acid (**1a**) and 4-*O*-β-D-glucuronylferulic acid (**5b**) gave K_1 values significantly weaker than the lower limit (15×10^3 M^{-1}) determined from the quenching of HSA fluorescence, which is indicative of possible noncompetitive binding. Hence, glucuronidation, or even a more minor structural change such as an additional methoxy group, is enough to induce a substantial move of the ligand within sub-domain IIA.

Finally, **5a** acid barely lowers the fluorescence of the quercetin–HSA complex at 530 nm. The corresponding I_F *vs.* L_t curve remains much higher than the theoretical curve assuming competitive binding and construction from $K_1 \approx 22 \times 10^3$ M^{-1} for the ligand–HSA complex and 222×10^3 M^{-1} for the quercetin–HSA complex, and from the values for the molar fluorescence intensity of free and HSA-bound quercetin ($f_Q \approx 4290$ M^{-1}, $f_{QP} \approx 3 \times 10^5$ M^{-1} at 530 nm) (Fig. 5). It can thus be concluded that the bindings of 4-*O*-β-D-glucuronyl-*p*-coumaric acid and quercetin are noncompetitive. Unlike competition with the dansyl probes, this behaviour appears fairly general in the series of HCAs investigated. The fact that the dansyl probes, despite their relatively high affinity for HSA, only weakly quench the fluorescence of bound quercetin (data not shown) is also consistent with their binding to HSA noncompetitively with quercetin.[22]

In conclusion, hydroxycinnamic acids and their *O*-arylglucuronides moderately bind HSA in the IIA-domain ($K_1 = 1$–4×10^4 M^{-1}). Their interaction with HSA is clearly noncompetitive with quercetin and either competitive or noncompetitive with DNSS and DNSA. The moderate affinity of HCA glucuronides for HSA should be large enough to ensure substantial *in vivo* binding given the high concentration of HSA in plasma (*ca.* 0.6 mM) and the low concentrations of circulating polyphenol metabolites (<1 μM).

Experimental

Chemicals

p-Coumaric acid, ferulic acid, caffeic acid, quercetin, dansylamide (DNSA), dansylsarcosine (DNSS), glucurono-3,6-lactone and HSA (fraction V, MM = 66500 g mol^{-1}) were all purchased from Sigma-Aldrich. Glucuronyl donor **2** was synthesized from glucurono-3,6-lactone according to a 3-step procedure already described in the literature.[17,30] Methyl *p*-coumarate, ferulate and caffeate (**1a–1c**) were prepared as already reported.[18]

Analyses

^{1}H- and ^{13}C-NMR spectra were recorded on a 300 MHz Bruker apparatus at 27 °C. Chemical shifts (δ) are given in ppm (solvent as the internal reference), coupling constants (J) are given in Hz. High-resolution mass analyses were carried out on Qstar Elite instrument (Applied Biosystems SCIEX, Foster City, USA) equipped with API. Mass detection was performed in the negative or positive electrospray ionization mode. Steady-state fluorescence spectra were recorded on a thermostatted Safas Xenius spectrofluorometer. The excitation and emission slit widths were set at 10 nm. All studies were performed at 25 (± 1) °C. Two types of excitation–emission conditions were used: a) excitation at 335 or 360 nm (4-*O*-β-D-glucuronyl-*p*-coumaric acid and dansyl probes, respectively), emission light collected between 350 and 530 nm; or b) excitation at 295 nm (HSA Trp residue), emission light collected between 260 and 400 nm.

Chemical syntheses

Compound 3a. $BF_3{\cdot}Et_2O$ (2 equiv.‡) was added to a solution of **1a** (1 mmol) and **2** (2 equiv.) in dry CH_2Cl_2 (4 ml) under N_2 in the presence of 4 Å molecular sieves. The mixture was stirred at room temperature for 1 h, then concentrated and directly subjected to chromatography on silica gel (eluent AcOEt–C_6H_{12}, 3 : 7) to afford **3a**. R_f(AcOEt–C_6H_{12}, 6 : 4) = 0.53, yield 43%. ^{1}H-NMR ($CDCl_3$): 7.66 (1H, d, J = 15.9, H_β), 7.50 (2H, d, J = 8.7, H_2, H_6), 7.02 (2H, d, J = 8.7, H_3, H_5), 6.36 (1H, d, J = 15.9, H_α), 5.39–5.31 (3H, m, $H_{2'}$, $H_{3'}$, $H_{4'}$), 5.21 (1H, d, J = 6.9, $H_{1'}$), 4.23 (1H, d, J = 9.3, $H_{5'}$), 3.82 (3H, s, CO_2CH_3), 3.75 (3H, s, CO_2CH_3 (GlcU)), 2.08–2.06 (9H, 3 s, 3 $OCOCH_3$). ^{13}C-NMR ($CDCl_3$): 170.5, 169.7, 169.6, 167.2 (2 CO_2CH_3, 3 $OCOCH_3$), 158.4 (C_4), 144.3 (C_β), 130.0 (C_2, C_6), 128.3 (C_1), 117.6, 117.2 (C_3, C_5, C_α), 99.0 ($C_{1'}$), 73.1, 72.1, 71.4, 69.4 ($C_{2'}$, $C_{3'}$, $C_{4'}$, $C_{5'}$), 53.4–52.1 (2 $COOCH_3$), 21.0 (3 $OCOCH_3$). The NMR data of **3a** are consistent with the literature.[17]

Compound 3b. Same procedure as for **3a**. R_f(AcOEt–C_6H_{12}, 6 : 4) = 0.56, yield 84%. ^{1}H-NMR ($CDCl_3$): 7.63 (1H, d, J = 15.9, H_β), 7.11 (3H, m, H_2, H_5, H_6), 6.36 (1H, d, J = 15.9, H_α), 5.36–5.30 (3H, m, $H_{2'}$, $H_{3'}$, $H_{4'}$), 5.10 (1H, d, J = 6.9, $H_{1'}$), 4.13 (1H, d, J = 9.3, $H_{5'}$), 3.86, 3.82, 3.76 (9H, 3 s, 3 OCH_3), 2.10–2.05 (9H, 3 s, 3 $OCOCH_3$). ^{13}C-NMR ($CDCl_3$): 170.5, 169.7, 167.8, 159.6 (2 CO_2CH_3, 3 $OCOCH_3$), 151.2, 147.9, 144.6 (C_3, C_4, C_β), 131.5 (C_1), 120.4 (C_6), 117.6, 117.4 (C_α, C_5), 111.9 (C_2), 100.7 ($C_{1'}$), 73.1, 72.1, 71.4, 69.6 ($C_{2'}$, $C_{3'}$, $C_{4'}$, $C_{5'}$), 56.5 (OCH_3), 53.4, 52.1 (2 CO_2CH_3), 21.1, 20.9 (3 $OCOCH_3$).

‡ Concentration not optimized: a catalytic amount could suffice.[17,31]

Compounds 3c–3d. Same procedure as for **3a** except for the concentrations of $BF_3{\cdot}Et_2O$ and **2** (1 equiv.). The two regioisomers were isolated together. R_f(AcOEt–C_6H_{12}, 6 : 4) = 0.62, yield 35%. ^{1}H-NMR ($CDCl_3$): 7.59 (1H, d, J = 15.9, H_β), 7.27–6.96 (3H, m, H_2, H_5, H_6), 6.28 (1H, d, J = 15.9, H_α), 5.60–4.80 (3.4 H, m, $H_{1'}$, $H_{2'}$, $H_{3'}$, $H_{4'}$), 4.61 (0.6 H, d, J = 9.9, $H_{1'}$), 4.24 (1H, d, J = 9.0, $H_{5'}$), 3.81–3.76 (6H, m, 2 CO_2CH_3), 2.14–2.05 (9H, m, 3 $OCOCH_3$). ^{13}C-NMR ($CDCl_3$): 170.8, 170.2, 168.3, 167.5 (2 CO_2CH_3, 3 $OCOCH_3$), 150.3–148.3–145.5 (C_4, C_3, C_β), 132.4–128.0–126.7 (C_1, C_2, C_6), 118.3 (C_5), 116.7 (C_α), 91.0 ($C_{1'}$), 73.4, 72.0, 71.9, 69.7 ($C_{2'}$, $C_{3'}$, $C_{4'}$, $C_{5'}$), 54.0, 52.5 (2 CO_2CH_3), 21.5 (3 $OCOCH_3$).

4-*O*-β-D-Glucuronyl-*p*-coumaric acid (5a). **3a** (0.5 mmol) was stirred in 1 M NaOH (8 equiv.)–MeOH–H_2O (1 : 3 : 2) (24 ml) at room temperature for 15 h. After acidification with a proton-exchange resin and concentration, **5a** was isolated. R_f(CH_2Cl_2–MeOH, 1 : 1) = 0.32, yield 95%. ^{1}H-NMR (CD_3OD): 7.65 (1H, d, J = 15.9, H_β), 7.58 (2H, d, J = 8.7, H_2, H_6), 7.13 (2H, d, J = 8.7, H_3, H_5), 6.39 (1H, d, J = 15.9, H_α), 5.07 (1H, d, J = 7.8, $H_{1'}$), 4.04 (1H, d, J = 9.6, $H_{5'}$), 3.64–3.52 (3H, m, $H_{2'}$, $H_{3'}$, $H_{4'}$). ^{13}C-NMR (CD_3OD): 171.5 ($C_{6'}$), 169.9 (CO_2H), 145.2 (C_4, C_β), 130.2 (C_2, C_6), 130.1 (C_1), 117.3, 117.0 (C_3, C_5, C_α), 101.2 ($C_{1'}$), 76.4, 76.3, 73.9, 72.3 ($C_{2'}$, $C_{3'}$, $C_{4'}$, $C_{5'}$). HRMS: m/z 339.0718 ([M − H]$^-$) (339.0722, calcd for $C_{15}H_{16}O_9$). $[\alpha]_D$−72.1 (c 1, MeOH).

Compound 4b. **3b** (0.6 mmol) was stirred in MeOH (30 ml) containing *ca.* 0.1 equiv. MeONa at room temperature for 24 h. After acidification with a proton-exchange resin, concentration and chromatography on silica gel (eluent AcOEt), **4b** was isolated. R_f(AcOEt) = 0.15, yield 64%, melting point 180–181 °C. ^{1}H-NMR (CD_3OD): 7.66 (1H, d, J = 15.9, H_β), 7.29–7.20 (3H, m, H_2, H_5, H_6), 6.50 (1H, d, J = 15.9, H_α), 4.96 (1H, $H_{1'}$, masked by water signal), 3.91–3.37 (13H, m + 3 s, $H_{2'}$, $H_{3'}$, $H_{4'}$, $H_{5'}$ + 3 OCH_3). ^{13}C-NMR (CD_3OD): 172.6 ($C_{6'}$), 167.3, 155.3 (CO_2CH_3), 149.2 (C_β), 135.1, 127.4, 126.4, 122.6 (C_1, C_2, C_4, C_6), 121.0, 117.1, 115.8 (C_3, C_5, C_α), 103.0 ($C_{1'}$), 74.2, 70.4 ($C_{2'}$, $C_{3'}$, $C_{4'}$, $C_{5'}$), 59.9, 56.2, 55.4 (3 OCH_3).

Compounds 4c–4d. Same procedure as for **4b**. R_f(AcOEt) = 0.2, yield 50%. ^{1}H-NMR (CD_3OD): 7.60 (0.6H, d, J = 15.9, $H_{\beta(4d)}$), 7.58 (0.4H, d, J = 15.9, $H_{\beta(4c)}$), 7.44 (0.6H, d, J = 2.1, $H_{2(4d)}$), 7.21 (0.6H, dd, J = 2.1 and J = 8.4, $H_{6(4d)}$), 7.13 (0.4H, d, J = 2.1, $H_{2(4c)}$), 7.12 (0.4H, d, J = 8.4, $H_{5(4c)}$), 7.05 (0.4H, dd, J = 2.1, J = 8.4, $H_{6(4c)}$), 6.89 (0.6H, d, J = 8.4, $H_{5(4d)}$), 6.38 (0.4H, d, J = 15.9, $H_{\alpha(4c)}$), 6.34 (0,6H, d, J = 15.9, $H_{\alpha(4d)}$), 4.96 (0.4H, d, J = 7.5, $H_{1'(4c)}$), 4.95 (0.6H, d, J = 7.5, $H_{1'(4d)}$), 4.10 (0.6H, d, J = 9.6, $H_{5'(4d)}$), 4.07 (0.4H, d, J = 9.6, $H_{1'(4c)}$), 3.83 (1.8H, s, $OCH_{3(4d)}$), 3.80 (1.2H, s, $OCH_{3(4c)}$), 3.78 (3H, s, $OCH_{3(GlcU)}$), 3.73–3.51 (3H, m, $H_{2'}$, $H_{3'}$, $H_{4'}$).

4-*O*-β-D-Glucuronylferulic acid (5b). **4b** (0.5 mmol) was stirred in 1 M NaOH (2 equiv.)–MeOH–H_2O (1 : 3 : 2) (6 ml) at room temperature for 15 h. After acidification with a proton-exchange resin and concentration, **5b** was isolated. R_f(C18-silica gel, 0.05% aq. HCO_2H–MeCN, 1 : 1) = 0.89, yield 80%. ^{1}H-NMR (CD_3OD): 7.64 (1H, d, J = 15.9, H_β), 7.28–7.18 (3H, m, H_2, H_5, H_6), 6.42 (1H, d, J = 15.9, H_α), 5.06 (1H, d, J = 7.5, $H_{1'}$), 3.99 (1H, d, J = 9.6, $H_{5'}$), 3.92 (3H, s, OCH_3), 3.67–3.52 (3H, m, $H_{2'}$, $H_{3'}$, $H_{4'}$). ^{13}C-NMR (CD_3OD): 171.5 ($C_{6'}$), 169.9 (CO_2H), 150.6, 149.0, 145.4 (C_β, C_3, C_4), 130.4, 122.6, 117.4, 117.2, 112.0 (C_1, C_2, C_5, C_6, C_α),

101.7 ($C_{1'}$), 76.6, 76.0, 73.9, 72.3 ($C_{2'}$, $C_{3'}$, $C_{4'}$, $C_{5'}$), 55.3 (OCH_3). HRMS: m/z 369.0825 ($[M - H]^-$) (369.0828, calcd for $C_{16}H_{18}O_{10}$). $[\alpha]_D$ −19.9 (c 1, MeOH).

4-*O*-β-D-Glucuronylcaffeic acid (5c) and 3-*O*-β-D-glucuronylcaffeic acid (5d). Same procedure as for **5b**. R_f(C18 silica gel, 0.05% aq. HCO_2H–MeCN, 1 : 1) = 0.77, yield 80%. **5c** and **5d** were separated by semi-preparative chromatography on C18 silica gel (eluent 0.05% aq. HCO_2H–MeOH 9 : 1 to pure MeOH).

Data for **5c**: ^{1}H-NMR (CD_3OD): 7.58 (1H, d, J = 15.9, H_β), 7.17 (1H, d, J = 8.4, H_5), 7.13 (1H, d, J = 2.1, H_2), 7.06 (1H, dd, J = 8.4 and J = 2.1, H_6), 6.34 (1H, d, J = 15.9, H_α), 4.94 (1H, d, J = 7.2, $H_{1'}$), 4,00 (1H, d, J = 9.6, $H_{5'}$), 3.64–3.53 (3H, m, $H_{2'}$, $H_{3'}$, $H_{4'}$). ^{13}C-NMR (CD_3OD): 169.9 (2 CO_2H), 148.0, 147.9, 145.4 (C_β, C_3, C_4), 130.9, 121.4, 117.7, 117.3, 115.5 (C_1, C_2, C_5, C_6, C_α), 103.0 ($C_{1'}$), 76.3, 76.0, 73.8, 72.4 ($C_{2'}$, $C_{3'}$, $C_{4'}$, $C_{5'}$). HRMS: m/z 357.0815 ($[M + H]^+$), 374.1077 ($[M + NH_4]^+$) (357.0816, 374.1081, calcd for $C_{16}H_{18}O_{10}$). $[\alpha]_D$ −84.4 (c 1, MeOH).

Data for **5d**: ^{1}H-NMR (CD_3OD): 7.59 (1H, d, J = 15.9, H_β), 7.47 (1H, d, J = 2.1, H_2), 7.22 (1H, dd, J = 8.1 and J = 2.1, H_6), 6.90 (1H, d, J = 8.1, H_5), 6.31 (1H, d, J = 15.9, H_α), 4.92 (1H, d, J = 7.2, $H_{1'}$), 4.03 (1H, d, J = 9.6, $H_{5'}$), 3.65–3.54 (3H, m, $H_{2'}$, $H_{3'}$, $H_{4'}$). ^{13}C-NMR (CD_3OD): 171.7 ($C_{6'}$), 170.2 (CO_2H), 150.6, 146.1, 145.7 (C_β, C_3, C_4), 127.4, 125.6, 117.9, 117.0 (C_1, C_2, C_5, C_6), 115.9 (C_α), 103.7 ($C_{1'}$), 76.4, 75.9, 73.9, 72.3 ($C_{2'}$, $C_{3'}$, $C_{4'}$, $C_{5'}$). HRMS: m/z 357.0814 ($[M + H]^+$), 374.1080 ($[M + NH_4]^+$) (357.0816, 374.1081, calcd for $C_{16}H_{18}O_{10}$). $[\alpha]_D$ −73.4 (c 1, MeOH).

Fluorescence measurements

Solutions were prepared daily by dissolving HSA in a pH 7.4 buffer (50 mM phosphate–100 mM NaCl).

Interaction of albumin with a single ligand. Small aliquots (1–80 μL) of a concentrated ligand solution in MeOH or in MeOH–DMSO (9 : 1) were added *via* syringe to 2 mL of a 3.75 μM HSA solution placed in a quartz cell (path length: 1 cm). In all experiments, the maximal cosolvent concentration was 5%.

Interaction of albumin with a dansyl probe and a second ligand. To 2 mL of a 75 μM HSA solution were successively added 20 μL of a 7.5 mM solution of the dansyl probe in MeOH (1 : 1 HSA–probe molar ratio) and aliquots (1–300 μL) of a concentrated solution of the second ligand in MeOH or MeOH–DMSO (9 : 1).

Binding data treatment

All calculations were carried out with the least-square regression program Scientist (MicroMath, Salt Lake City, USA). Standard deviations and correlation coefficients are reported. Beside the expression of the fluorescence intensity I_F, the typical relationships used in the curve-fitting procedures were combinations of the mass law for the complexes and mass conservation for the ligand L, protein P and dansyl probes D (see below).

Fluorescence of the ligands in the presence of HSA. The excitation wavelength was selected so as to maximize the fluorescence of the bound ligand or probe (4-*O*-β-D-glucuronyl-*p*-coumaric acid, DNSA, DNSS). Assuming 1 : 1 binding, optimized values for the binding constant (K_1) and the molar fluorescence intensity of the complex (f_{PL}) were estimated by fitting the I_F *vs.* L_t curves against eqns (1)–(3) where L_t is the total ligand concentration and C the total protein concentration. The molar fluorescence intensity of the free ligand (f_L) was estimated from a linear plot of the fluorescence intensity *vs.* ligand concentration in the absence of HSA. The weak fluorescence intensity of free HSA (molar fluorescence intensity f_P) detected in the absence of ligand was taken into account.

$$I_F = f_L[L] + f_P[P] + f_{PL}K_1[L][P] \quad (1)$$

$$L_t = [L](1 + K_1[P]) \quad (2)$$

$$C = [P](1 + K_1[L]) \quad (3)$$

Quenching of the intrinsic fluorescence of HSA by the ligands. The excitation wavelength was selected so as to maximize the fluorescence of the single Trp residue of HSA. However, most ligands substantially absorb light at the excitation wavelength (295 nm) so that an inner filter correction is necessary. Hence, the protein fluorescence intensity is expressed as eqn (4), which is used with eqn (2) and eqn (3) in the curve-fitting procedure.

$$I_F = f_P[P]\exp(-\varepsilon_L l L_t) \quad (4)$$

In eqn (4), ε_L stands for the molar absorption coefficient of the ligand at the excitation wavelength, and has been checked to be identical for the bound or free ligand. Its value is determined independently by UV-visible spectroscopy from a Beer's plot. Finally, l is the mean distance travelled by the excitation light at the site of emission light detection. For the spectrometer used in this work, l is estimated to be 0.65 cm.

When necessary, additional 1 : 2 protein-ligand binding (stepwise binding constant K_2) was taken into account, leading to eqns (5)–(7):

$$L_t = [L] + K_1[P][L] + K_1K_2[P][L]^2 \quad (5)$$

$$C = [P](1 + K_1[L] + K_1K_2[L]^2) \quad (6)$$

$$I_F = [P](f_P + f_{PL}K_1[L])\exp(-\varepsilon_L l L_t) \quad (7)$$

In eqn (7), the fluorescence of complex PL_2 is neglected.

Quenching of the fluorescence of dansyl probe–HSA complexes by the ligands. The excitation wavelength was selected so as to maximize the fluorescence of the bound probe. Assuming competition between the dansyl probe D and ligand L and pure 1 : 1 binding, eqns (8) and (9) can be derived and used in the curve-fitting of the I_F *vs.* L_t curve for the determination of optimized values for parameters K_1 and f_{DP} (after preliminary determination of K_D in the absence of L and of f_D in the absence of L and P).

$$I_F = D_t\frac{f_D + f_{DP}K_D[P]}{1 + K_D[P]}\exp(-\varepsilon_L l L_t) \quad (8)$$

$$C = [P]\left(1 + \frac{K_D D_t}{1 + K_D[P]} + \frac{K_1 L_t}{1 + K_1[P]}\right) \quad (9)$$

where f_D and f_{DP} are the molar fluorescence intensities of the dansyl probe and dansyl probe–albumin complex, respectively, D_t is the total concentration of the dansyl probe, K_D the probe–HSA binding constant and ε_L the molar absorption coefficient of the ligand at the excitation wavelength.

References

1 M. Clifford and J. E. Brown, in: *Flavonoids: Chemistry, Biochemistry & Applications*, ed. O. Andersen and K. Markham, CRC Press, Boca Raton, 2006, pp. 319–370.
2 C. Manach, G. Williamson, C. Morand, A. Scalbert and C. Remesy, *Am. J. Clin. Nutr.*, 2005, **81**, 230S–242S.
3 S. Lafay, A. Gil-Izquierdo, C. Manach, C. Morand, C. Besson and A. Scalbert, *J. Nutr.*, 2006, **136**, 1192–1197.
4 Y. Konishi, Y. Hitomi and E. Yoshioka, *J. Agric. Food Chem.*, 2004, **52**, 2527–2532.
5 Y. Konishi and S. Kobayashi, *J. Agric. Food Chem.*, 2004, **52**, 2518–2526.
6 S. M. Kern, R. N. Bennett, P. W. Needs, F. A. Mellon, P. A. Kroon and M. T. Garcia-Conesa, *J. Agric. Food Chem.*, 2003, **51**, 7884–7891.
7 K. Azuma, K. Ippoushi, M. Nakayama, H. Ito, H. Higashio and J. Terao, *J. Agric. Food Chem.*, 2000, **48**, 5496–5500.
8 M. Nardini, E. Cirillo, F. Natella and C. Scaccini, *J. Agric. Food Chem.*, 2002, **50**, 5735–5741.
9 S. M. Kern, R. N. Bennett, F. A. Mellon, P. A. Kroon and M. T. Garcia-Conesa, *J. Agric. Food Chem.*, 2003, **51**, 6050–6055.
10 M. Nardini, F. Natella, C. Scaccini and A. Ghiselli, *J. Nutr. Biochem.*, 2006, **17**, 14–22.
11 L. C. Bourne and C. Rice-Evans, *Biochem. Biophys. Res. Commun.*, 1998, **253**, 222–227.
12 O. Dangles, C. Dufour, C. Manach, C. Morand and C. Remesy, *Methods Enzymol.*, 2001, **335**, 319–333.
13 T. Peters, *All about albumin: biochemistry, genetics and biomedical applications*, Academic Press, San Diego, 1996.
14 C. Dufour, M. Loonis and O. Dangles, *Free Radical Biol. Med.*, 2007, **43**, 238–250.
15 K. M. Janisch, G. Williamson, P. Needs and G. W. Plumb, *Free Radical Res.*, 2004, **38**, 877–884.
16 A. V. Stachulski, J. R. Harding, J. C. Lindon, J. L. Maggs, B. K. Park and I. D. Wilson, *J. Med. Chem.*, 2006, **49**, 6931–6945.
17 A. G. Pearson, M. J. Kiefel, V. Ferro and M. V. Itzstein, *Carbohydr. Res.*, 2005, **340**, 2077–2085.
18 S. Galland, N. Mora, M. Abert-Vian, N. Rakotomanomana and O. Dangles, *J. Agric. Food Chem.*, 2007, **55**, 7573–7579.
19 D. W. Boulton, U. K. Walle and T. Walle, *J. Pharm. Pharmacol.*, 1998, **50**, 243–249.
20 F. Zsila, Z. Bikadi and M. Simonyi, *Biochem. Pharmacol.*, 2003, **65**, 447–456.
21 B. Sengupta and P. K. Sengupta, *Biochem. Biophys. Res. Commun.*, 2002, **299**, 400–403.
22 C. Dufour and O. Dangles, *Biochim. Biophys. Acta*, 2005, **1721**, 164–173.
23 C. Manach, C. Morand, V. Crespy, C. Demigne, O. Texier, F. Regerat and C. Remesy, *FEBS Lett.*, 1998, **426**, 331–336.
24 D. E. Epps, T. J. Raub, V. Caiolfa, A. Chiari and M. Zamai, *J. Pharm. Pharmacol.*, 1999, **51**, 41–48.
25 B. Valeur, *Molecular fluorescence*, Wiley-VCH, Weinheim, 2002.
26 J. Ghuman, P. A. Zunszain, I. Petitpas, A. A. Bhattacharya, M. Otagiri and S. Curry, *J. Mol. Biol.*, 2005, **353**, 38–52.
27 J. Min, X. Meng-Xia, Z. Dong, L. Yuan, L. Xiao-Yu and C. Xing, *J. Mol. Struct.*, 2004, **692**, 71–80.
28 J. Kang, Y. Liu, M.-X. Xie, S. Li, M. Jiang and Y.-D. Wang, *Biochim. Biophys. Acta*, 2004, **1674**, 205–214.
29 D. E. Epps, T. J. Raub and F. J. Kezdy, *Anal. Biochem.*, 1995, **227**, 342–350.
30 B. Fischer, A. Nudelman, M. Ruse, J. Herzig, H. E. Gottlieb and E. Keinan, *J. Org. Chem.*, 1984, **49**, 4988–4993.
31 R. T. Brown, F. Scheinmann and A. V. Stachulski, *J. Chem. Res. (S)*, 1997, 370–371.

